

This is a provisional PDF only. Copyedited and fully formatted version will be made available soon.

REPORTS OF PRACTICAL ONCOLOGY AND RADIOTHERAPY

ISSN: 1507-1367

e-ISSN: 2083-4640

Effect of internal port on dose distribution in post-mastectomy radiotherapy for breast cancer patients after expander breast reconstruction

Authors: Elisabetta Perrucci, Marta Marcantonini, Eleonora Arena, Christian Fulcheri, Valentina Reggioli, Anna Concetta Dipilato, Isabella Palumbo, Simonetta Saldi, Lorenzo Falcinelli, Gianluca Ingrosso, Vittorio Bini, Cynthia 5 Aristei

DOI: 10.5603/RPOR.a2023.0014

Article type: Research paper

Published online: 2023-03-21

This article has been peer reviewed and published immediately upon acceptance. It is an open access article, which means that it can be downloaded, printed, and distributed freely, provided the work is properly cited.

Effect of internal port on dose distribution in post-mastectomy radiotherapy for breast cancer patients after expander breast reconstruction

10.5603/RPOR.a2023.0014

Elisabetta Perrucci¹, Marta Marcantonini², Eleonora Arena³, Christian Fulcheri², Valentina Reggioli², Anna Concetta Dipilato⁴, Isabella Palumbo⁴, Simonetta Saldi¹, Lorenzo Falcinelli¹, Gianluca Ingrosso⁴, Vittorio Bini⁵, Cynthia Aristei⁴

¹*Radiation Oncology Section, Perugia General Hospital, Perugia, Italy*

²*Medical Physics Unit, Perugia General Hospital, Perugia, Italy*

³*Radiotherapy Department, State Hospital, Ancona, Italy*

⁴*Radiation Oncology Section, University of Perugia and Perugia General Hospital, Perugia, Italy*

⁵*Department of Medicine, Section of Internal Medicine and Endocrine and Metabolic Sciences, University of Perugia, Perugia, Italy*

Corresponding author: Elisabetta Perrucci, Radiation Oncology Section, Perugia General Hospital, P.le G. Menghini 8-9, 06156 Perugia, Italy, tel/fax: +390755783614, e-mail elisabetta.perrucci@ospedale.perugia.it

Abstract

Background: In patients with expander-based reconstruction a few dosimetric analyses detected radiation therapy dose perturbation due to the internal port of an expander, potentially leading to toxicity or loss of local control. This study aimed at adding data on this field.

Materials and methods: A dosimetric analysis was conducted in 30 chest wall treatment planning without and with correction for port artifact. In plans with artifact correction density was overwritten as 1 g/cm³. Medium, minimum and maximum chest wall doses were compared in the two plans. Both plans, with and without correction, were compared on an anthropomorphic phantom with a tissue expander on the chest covered by a *bolus* simulating the skin. *Ex vivo*

dosimetry was carried out on the phantom and *in vivo dosimetry* in three patients by using film strips during one treatment fraction. Estimated doses and measured film doses were compared.

Results: No significant differences emerged in the minimum, medium and maximum doses in the two plans, without and with correction for port artifacts. *Ex vivo* and *in vivo* analyses showed a good correspondence between detected and calculated doses without and with correction.

Conclusions: The port did not significantly affect dose distribution in patients who will receive post-mastectomy radiation therapy (PMRT).

Key words: postmastectomy radiotherapy; breast reconstruction; internal port; dose distribution

Introduction

Around 30% of patients with newly diagnosed breast cancer receive mastectomy and are generally offered breast reconstruction to improve quality of life [1]. Even though post-mastectomy radiation therapy (PMRT), as part of a multi-modality approach, reduced the risk of loco-regional relapse and improved survival in locally advanced or early stage positive node disease [1, 2], it was linked to a high rate of complications, particularly in cases with expander/implant reconstruction [3–7]. Complications included severe capsular contracture, infections, implant distortion or loss, pain and poor cosmetic outcome [1–5]. Acute complications can, furthermore, interrupt the scheduled treatment for some or even many days. If the break is longer than 1 week it may be associated with less local disease control and, thus, impact upon survival [8].

Other concerns are related to expander irradiation which over half of breast cancer patients underwent before the permanent breast implant exchange [9]. In about 60% of cases, expanders in the sub-pectoral muscle have an internal port for saline solution injection to expand the overlying chest wall tissues [10]. The port contains a rare-earth magnet that produces an artifact in computerized tomography (CT) images which, in turn, affects dose distribution, increasing the risk of an overdose which could cause complications, or an under-dose which could reduce local disease control [11, 12].

Few *ex vivo* dosimetric analyses addressed the effect of the internal magnetic port on radiation dose attenuation by means of film and thermoluminescent dosimeters. Using a single beam, the dose reduction behind the port varied with beam orientation and energy [12–14]. Although the dose was slightly increased at the edge of the magnet due to radiation backscatter, the increase may be of little clinical significance as it was restricted to the silicone envelope [13, 14].

Monte Carlo simulation with 2 tangential beams to mimic the clinical setting provided conflicting results. Compared with irradiation without an expander, Chatzigiannis et al. [15] found the absorbed dose reduction in the port shadow ranged from 7% to 13% for 6 MV photons and was around 6% for 18 MV photons. On the other hand, Trombetta et al. [16] did not find any significant changes with 2 opposed 6 MV photon beams, while a 7% under-dose was found with a single beam.

Dosimetric evaluation of plans with and without correction for the rare-earth magnet electron density showed that on corrected plans dose heterogeneity was increased and the dose to the clinical target volume (CTV) was reduced, particularly around the magnet [17]. However, in *in vivo* dosimetry studies, Gee et al. using 2 opposed 6 MV photon beams reported a 7% skin dose reduction in the port shadow in 15/16 patients [18], but Damast et al. found the dose was reduced significantly in only 1/6 patients using tangential 15-MV photon beams [13].

Given these discrepancies, the present study compared dosimetry in real clinical plans (RP) without any corrections for 30 patients who were treated at our Radiation Oncology Unit and plans with port artifact correction (corrected plans, CP). Furthermore, RP and CP were made and results compared in an anthropomorphic phantom with an expander and then *ex vivo* dosimetry was carried out. Finally, *in vivo* dosimetry was performed in 3 patients and results were compared with the corresponding doses as achieved in the RP and CP. Figure 1 shows the study design.

Materials and methods

Thirty post-mastectomy breast cancer patients who underwent breast reconstruction with a temporary tissue expander received 3D conformal PMRT. Target volumes were the chest wall in all patients and the draining nodes in 27 of them. All had given their informed consent to their data being used in this study. Breast reconstruction was performed with Natrelle 133® (ALLERGAN, Santa Barbara, CA), a silicone elastomer expansion envelope with a textured surface and a MAGNA-SITE™ integrated injection site. It contains a rare-earth permanent magnet disk (Nd₂Fe₁₄B; Neodymium magnet, nominal density = 7.4 g/cm³) which is 2.1 cm in diameter and 3.5 mm in thickness. The magnet is cased in a titanium shell (3.5 cm in diameter and 0.4 mm in thickness) with a nominal density of 4.2 g/cm³. The MAGNA-FINDER™ external locating device indicates the MAGNA-SITE™ location.

All patients underwent CT simulation with 3 mm slice thickness for PMRT planning. The target volumes were contoured on every slice according to the guidelines of the Italian Association of Radiotherapy and Clinical Oncology (Associazione Italiana di Radioterapia ed Oncologia Clinica; AIRO) [19]. RP were generated in the Pinnacle treatment planning system (TPS) V9.8 (Philips

Radiation Oncology Systems, Fitchburg, WI, United States). The prescribed dose was 50 Gy in 25 fractions, with standard fractionation. No skin *bolus* was used for any patient. Doses were modulated using two opposite tangential co-planar beams with the field-in-field technique. Virtual wedges were used. In order to speed up the optimization task a dose grid of 4 x 4 x 4 mm³ was first used in combination with the Adaptive Convolve dose engine for manual plan optimization. Then a 2x2x2 mm³ dose grid resolution was combined with the Collapsed Cone Convolution dose engine (the most accurate dose algorithm used by Pinnacle) to calculate the final dose. No corrections for port heterogeneity were performed on RP. International Commission on Radiation Units and Measurements (ICRU) 62 recommendations [20] were used for dose goals to the planning target volumes (PTV) and QUANTEC recommendations [21] for dose constraints to organs at risk (OARs). All treatments were delivered using a 6 MV linear accelerator.

CP were calculated for all patients in order to correct the port artifact effect on dose distribution. The port was identified by setting a “bone-like” window width and level from 1000 to 2000 (raw units) in the TPS, including also some of the image artifacts. The chest wall PTV was created without the port (PTV-port), by subtracting the port volume from target volume, and its density was corrected to 1 g/cm³ (saline solution). A non extended CT-density table, with a maximum density of 3.5 g/cm³, was used. The port structure was assigned the default density converted from the number read by the CT dataset.

Dosimetry was compared in the 30 RP and CP, considering the medium, minimum and maximum doses to the PTV and PTV-port, as reported in the TPS.

We then performed *ex vivo* and *in vivo* dosimetry at selected points chosen on the CT scan to assess port-related dose variations at skin level. They were compared with calculated doses in the corresponding RP and CP on TPS. For *ex vivo* dosimetry a Natrelle133 tissue expander covered by a 0.5 cm *bolus* simulating human skin was mounted on the Alderson Rando anthropomorphic phantom. As for any real patient, a CT scan was acquired, target contouring was performed by a radiation oncologist, RP and CP were calculated and dosimetric outcomes were compared. One radiotherapy fraction of RP was delivered to the phantom. To measure the delivered dose, 6 rectangular strips of radiochromic film EBT3 measuring approximately 2.5 cm x 2 cm (for easy handling) were positioned on the expander. After the port had been located by MAGNA-FINDER™, 3 films were put on the transversal line crossing the port while the other 3 were placed on the transversal line crossing radio-opaque marker alignment so as to easily identify their positions in the TPS plans. According to EBT3 usage recommendation, 24 hours lapsed between RT administration and the film scans, which was performed using an Epson scanner (version 3.49A).

The scanning parameters were: 48-bit color and 72 dpi resolution. The Film Analyzer program (TomoTherapy Hi-ART Software) converted film responses into dose using the appropriate calibration curve. A central region of interest (ROI) of about 2 mm x 2 mm was used to obtain the medium dose and its standard deviation at each center strip. All doses were compared with the RP and CP.

In vivo dosimetry was performed in 3 patients. Doses were measured during a treatment session using 6 radiochromic film EBT3 strips of 2.5 cm x 2 cm, as described above in *ex vivo* dosimetry. Three films were put on the transversal line crossing the port, as indicated by MAGNA-FINDER™ and another 3 were placed on the transversal line crossing the tattoo alignment on the reconstructed breast. Film doses were compared with the RP and CP calculated doses. Study design is shown in Fig 1.

Statistical analyses

The non parametric Wilcoxon signed rank test for paired data compared the calculated doses in the RP and PP for 30 patients and the *ex vivo* and *in vivo* dosimetry. The significance threshold was set at $p \leq 0.05$. All calculations were performed by using IBM-SPSS rel. 23.0, 2015.

Reproducibility, the degree to which different measurements provide similar results, was assessed in the three patients in whom *in vivo* dosimetry was performed. Measures of agreement and reliability quantified reproducibility.

Inter-observer agreement was quantified by calculating the mean difference between the measure modality pairs and the relative standard deviation (SD). Subsequently, the 95% limits of agreement were calculated according to the method of Bland and Altman [22], defined as the mean difference between the measure modalities $\pm 1.96*SD$.

Reliability: the intra-class correlation coefficient (ICC) was derived from a random-effects two-way analysis of variance (ANOVA). The ICC was defined as the ratio of the variance between patients over the total variance [23]. ICC is scaled as follows: 0–0.2 indicates poor agreement; 0.3–0.4 fair agreement; 0.5–0.6 moderate agreement; 0.7–0.8 strong agreement; and > 0.8 almost perfect agreement [24].

Results

The port structure volume including some of the image artifacts was in the range of 2.6–2.85 cm³. Minimum, medium and maximum PTV doses in the RP and CP were: 3.90 Gy (range 1.08–41.00 Gy) and 4.00 Gy (range 1.06–41.00 Gy), $p = 0.094$, for minimum doses; 48.35 Gy (range 44.39–

50.17 Gy) and 48.44 Gy (range 44.92–50.40 Gy), $p = 0.057$, for medium doses; 55.49 Gy (range 52.80–61.59 Gy) and 56.27 Gy (range 52.80–61.64 Gy), $p = 0.280$, for maximum doses. No significant differences emerged between RPs and CPs doses.

For results of *ex vivo* dosimetry and the RP and CP calculated doses on the phantom, doses measured with films were slightly higher at all points, except one. There, it was 8 cGy lower. Results of *ex vivo* dosimetry and the RP and CP calculated doses are shown in Supplementary File — Table S1.

Results of *in vivo* dosimetries and of the calculated RP and CP doses in the 3 patients are shown in Table 1. An excellent agreement emerged between film doses and calculated RP and CP TPS doses. Agreement between CP doses and film doses was better than that between RP doses and film doses (Tab. 2).

Discussion

Two-stage expander-implant breast reconstruction after mastectomy is widely used in clinical practice nowadays because it is a relatively easy procedure with low complications and is a more attractive option for patients and surgeons than autologous tissue procedures [25].

In the past, concerns about the safety and toxicity of PMRT after breast reconstruction were often expressed, particularly with expander-implant procedures [3–5, 26, 27]. More recent studies have reported good long-term outcomes and local control with no dose increase to the lung and heart [28, 29]. Concerns, however, persist about local disease control and toxicity because of potential dose perturbation, that could be caused by the rare-earth material in the internal port of the expander, as reported in dosimetric studies and *in vivo* evaluations [12–15, 17, 18].

Data are partially conflicting. Image artifacts lead to difficulties in port localization and the rare-earth material itself leads to inaccurate TPS dose calculation. Furthermore, dose accuracy estimations are linked to TPS features [13, 14, 30]. Data from a study using the Monte Carlo algorithm [15] suggested the absorbed dose was reduced in the port shadow and the reduction was even larger when lower beam energy was used. On the contrary, other dosimetric and *ex vivo* analyses did not report significant differences when 2 opposed beams were used, as is routine in clinical practice [11, 16]. *In vivo* dosimetry data were also divergent. Damast et al. [13] did not find dose decreases, while Gee et al. [18] observed a dose reduction in 15/16 patients in an average area of 1.07 cm², thus affecting only a small volume around the magnet. Consequently, port impact on overall dose distribution was probably of little dosimetric and clinical significance when tangent

irradiation was performed [11, 14, 16]. Nevertheless, measured dose reduction to the skin ranged from 4% to 10% [12, 14, 18]. In order to improve the dosimetric accuracy of treatment plans, a metallic port model was developed, validated and compared with 2 widely used clinical models which differed in the contouring modalities; the second one was very similar to the present one. Although the old clinical models overestimated or underestimated, respectively, the dose attenuation from the metallic port, results showed that for all plans and models the metal port had an impact which was significant for the skin but not for the chest wall. This effect was mainly observed for the 2 opposite field technique rather than for the VMAT and 4-field IMRT because of the higher number of beam angles with the latter techniques [31].

In the present dosimetric study on dose perturbation effect due to the port, we assigned a saline solution density to the artefacts caused by the rare earth (high Z) magnet, without applying any density override to the magnet itself. These choices were dictated by uncertainties as to the magnet's real density and inner structure and difficulties in accurately contouring it [30].

Our study defined the port density using a simpler method than Yoon et al. [31], but, because of it, over-estimated port volume as it comprised artifacts in our CP plans. We did not find any significant dose differences between the RP (with no correction) and the CP (which had been corrected for port artefact). However, since borderline significance emerged for the medium dose ($p = 0.057$), we are unable to establish whether our sample size of 30 plans could have determined the lack of significance. In any case, dose differences in the medium dose were so small (23 cGy) as to have a negligible clinical impact. Dose differences in our study were lower than reported by Chen et al. [17], who performed a dosimetric study with two different port density corrections. They found CTV coverage by the prescribed dose of 50 Gy was significantly lower in the CPs than in the plan without correction. Furthermore, the worst homogeneity and conformal dose distribution indices and CTV coverage were all found in the CPs [17].

With the aim of investigating port-related perturbation to the dose delivered during a treatment session, the present study performed film dosimetry on the phantom and on 3 patients. Although in *ex vivo* dosimetry measured doses were slightly higher than TPS calculated doses for both RP and PP, the dose differences at each point did not exceed 0.3 Gy for plans and films. Even in *in vivo* dosimetries the dose differences at each point did not exceed 0.3 Gy for plans and films.

It is worth noting that skin doses in our study were lower than the prescribed single dose of 2 Gy at each point in both plans and films. To ensure the skin is not under-dosed, as it could constitute a target in chest wall irradiation as in pT4b,c,d tumours, the use of *bolus* should be recommended, even after reconstruction [10]. Actually, in routine clinical practice, PMRT varies greatly with about

half of radiation oncologists never using bolus [10,32,33]. In accordance with our Radiotherapy Centre, the bolus was never used in the present study, as no disease stage and no other risk factors required higher skin dose. As previously reported, we observed good outcomes in terms of local control, survival and cosmesis in our patients [28]; in this group, acute toxicity was limited to mild-to-moderate skin toxicity which did not interrupt treatment.

PMRT guidelines after implant breast reconstruction were published [34]. PMRT as delivered with intensity modulated RT techniques, can lower toxicity and improve target coverage [35]. In fact, compared with three different modalities of intensity modulated irradiation, three-dimensional conformal radiation therapy (3D-CRT) provides the poorest coverage of complex shaped targets [35]. Moreover, the volumetric approach provides the additional benefit of excluding the implant/expander from the target, thus reducing the port effect on dose distribution.

The strength of our study lay in comparing 30 RP and 30 CP and in demonstrating there were no differences in dose distribution in plans that were uncorrected and corrected for the port. Film doses in *ex vivo* and *in vivo* dosimetries showed an excellent correspondence with calculated doses in both sets plans.

Despite the difficulty in assessing the superficial dose and the true internal port structure due to its artifacts, a good correlation emerged between TPS estimated doses and detected doses without any correction for the port. This result concurs with previous observations; using standard 3D irradiation, the port was reported to affect dose distribution only within its immediate area inside the expander, thus exerting no clinical effect [14, 16, 17].

Our results are in agreement with those of a recent study of Mayorov and Ali [17] where dosimetric impact of the metal port of tissue expanders was considered, along with the effect of the inter-fractional positional variations of the metal port itself, even if the strategy proposed to handle metallic port in planning is slightly different from that of the present study. Furthermore, daily positional variations of the metal port have small and not clinically relevant effects on target coverage and OARs.

Conclusions

In conclusion, present evidence reinforced previous findings [14, 16, 17] that the internal port, due to its small size, does not significantly affect the dose distribution in the CTV when tangential opposed beams are used. In particular, any area that resulted as under-dosed area, was very small and clinically negligible. Moreover, the presence of the port in patients with expander breast

reconstruction who undergo PMRT does not translate into a detrimental effect on toxicity and clinical outcomes [28, 29].

The most interesting point to emerge from the present study was the correspondence between TPS calculated doses, without and with port-related artefact correction, and the film doses detected during an irradiation session both in the phantom and *in vivo*. This correspondence was observed without correction for port density which is not easy to estimate.

Ethical permission

Ethical approval was not necessary for the preparation of this article

Funding

This publication was prepared without any external source of funding.

Conflict of interest

The authors have no conflict of interest to declare.

References

1. Walsh SM, Lowery AJ, Prichard RS, et al. Postmastectomy radiotherapy: indications and implications. *Surgeon*. 2014; 12(6): 310–315, doi: [10.1016/j.surge.2014.04.004](https://doi.org/10.1016/j.surge.2014.04.004), indexed in Pubmed: [25037652](https://pubmed.ncbi.nlm.nih.gov/25037652/).
2. Recht A, Comen EA, Fine RE, et al. Postmastectomy Radiotherapy: An American Society of Clinical Oncology, American Society for Radiation Oncology, and Society of Surgical Oncology Focused Guideline Update. *Pract Radiat Oncol*. 2016; 6(6): e219–e234, doi: [10.1016/j.prro.2016.08.009](https://doi.org/10.1016/j.prro.2016.08.009), indexed in Pubmed: [27659727](https://pubmed.ncbi.nlm.nih.gov/27659727/).
3. Jagsi R, Jiang J, Momoh AO, et al. Complications After Mastectomy and Immediate Breast Reconstruction for Breast Cancer: A Claims-Based Analysis. *Ann Surg*. 2016; 263(2): 219–227, doi: [10.1097/SLA.0000000000001177](https://doi.org/10.1097/SLA.0000000000001177), indexed in Pubmed: [25876011](https://pubmed.ncbi.nlm.nih.gov/25876011/).
4. Kung TA, Kidwell KM, Speth KA, et al. Impact of Radiotherapy on Complications and Patient-Reported Outcomes After Breast Reconstruction. *J Natl Cancer Inst*. 2018; 110(2): 157–165, doi: [10.1093/jnci/djx148](https://doi.org/10.1093/jnci/djx148), indexed in Pubmed: [28954300](https://pubmed.ncbi.nlm.nih.gov/28954300/).
5. Momoh AO, Ahmed R, Kelley BP, et al. A systematic review of complications of implant-based breast reconstruction with preconstruction and postreconstruction radiotherapy. *Ann Surg Oncol*. 2014; 21(1): 118–124, doi: [10.1245/s10434-013-3284-z](https://doi.org/10.1245/s10434-013-3284-z), indexed in Pubmed: [24081801](https://pubmed.ncbi.nlm.nih.gov/24081801/).
6. Poppe MM, Agarwal JP. Breast Reconstruction With Postmastectomy Radiation: Choices and Tradeoffs. *J Clin Oncol*. 2017; 35(22): 2467–2470, doi: [10.1200/JCO.2017.72.7388](https://doi.org/10.1200/JCO.2017.72.7388), indexed in Pubmed: [28481705](https://pubmed.ncbi.nlm.nih.gov/28481705/).
7. McGale P, Taylor C, Correa C, et al. EBCTCG (Early Breast Cancer Trialists' Collaborative Group). Effect of radiotherapy after mastectomy and axillary surgery on 10-year recurrence and 20-year breast cancer mortality: meta-analysis of individual patient data for 8135 women in 22 randomised trials. *Lancet*. 2014; 383(9935): 2127–2135, doi: [10.1016/S0140-6736\(14\)60488-8](https://doi.org/10.1016/S0140-6736(14)60488-8), indexed in Pubmed: [24656685](https://pubmed.ncbi.nlm.nih.gov/24656685/).

8. Bese NS, Sut PA, Ober A. The effect of treatment interruptions in the postoperative irradiation of breast cancer. *Oncology*. 2005; 69(3): 214–223, doi: [10.1159/000087909](https://doi.org/10.1159/000087909), indexed in Pubmed: [16127290](https://pubmed.ncbi.nlm.nih.gov/16127290/).
9. Thomas K, Rahimi A, Spangler A, et al. Radiation practice patterns among United States radiation oncologists for postmastectomy breast reconstruction and oncoplastic breast reduction. *Pract Radiat Oncol*. 2014; 4(6): 466–471, doi: [10.1016/j.prro.2014.04.002](https://doi.org/10.1016/j.prro.2014.04.002), indexed in Pubmed: [25407870](https://pubmed.ncbi.nlm.nih.gov/25407870/).
10. Chen SA, Hiley C, Nickleach D, et al. Breast reconstruction and post-mastectomy radiation practice. *Radiat Oncol*. 2013; 8: 45, doi: [10.1186/1748-717X-8-45](https://doi.org/10.1186/1748-717X-8-45), indexed in Pubmed: [23452558](https://pubmed.ncbi.nlm.nih.gov/23452558/).
11. Strang B, Murphy K, Seal S, et al. Does the presence of an implant including expander with internal port alter radiation dose? An ex vivo model. *Can J Plast Surg*. 2013; 21(1): 37–40, doi: [10.1177/229255031302100109](https://doi.org/10.1177/229255031302100109), indexed in Pubmed: [24431935](https://pubmed.ncbi.nlm.nih.gov/24431935/).
12. Moni J, Graves-Ditman M, Cederna P, et al. Dosimetry around metallic ports in tissue expanders in patients receiving postmastectomy radiation therapy: an ex vivo evaluation. *Med Dosim*. 2004; 29(1): 49–54, doi: [10.1016/j.meddos.2003.10.005](https://doi.org/10.1016/j.meddos.2003.10.005), indexed in Pubmed: [15023393](https://pubmed.ncbi.nlm.nih.gov/15023393/).
13. Damast S, Beal K, Ballangrud A, et al. Do metallic ports in tissue expanders affect postmastectomy radiation delivery? *Int J Radiat Oncol Biol Phys*. 2006; 66(1): 305–310, doi: [10.1016/j.ijrobp.2006.05.017](https://doi.org/10.1016/j.ijrobp.2006.05.017), indexed in Pubmed: [16904530](https://pubmed.ncbi.nlm.nih.gov/16904530/).
14. Thompson RCA, Morgan AM. Investigation into dosimetric effect of a MAGNA-SITE tissue expander on post-mastectomy radiotherapy. *Med Phys*. 2005; 32(6): 1640–1646, doi: [10.1118/1.1914545](https://doi.org/10.1118/1.1914545), indexed in Pubmed: [16013723](https://pubmed.ncbi.nlm.nih.gov/16013723/).
15. Chatzigiannis C, Lympelopoulou G, Sandilos P, et al. Dose perturbation in the radiotherapy of breast cancer patients implanted with the Magna-Site: a Monte Carlo study. *J Appl Clin Med Phys*. 2011; 12(2): 3295, doi: [10.1120/jacmp.v12i2.3295](https://doi.org/10.1120/jacmp.v12i2.3295), indexed in Pubmed: [21587170](https://pubmed.ncbi.nlm.nih.gov/21587170/).
16. Trombetta DM, Cardoso SC, Facure A, et al. Influence of the presence of tissue expanders on energy deposition for post-mastectomy radiotherapy. *PLoS One*. 2013; 8(2): e55430, doi: [10.1371/journal.pone.0055430](https://doi.org/10.1371/journal.pone.0055430), indexed in Pubmed: [23405149](https://pubmed.ncbi.nlm.nih.gov/23405149/).
17. Chen SA, Ogunleye T, Dhabbaan A, et al. Impact of internal metallic ports in temporary tissue expanders on postmastectomy radiation dose distribution. *Int J Radiat Oncol Biol Phys*. 2013; 85(3): 630–635, doi: [10.1016/j.ijrobp.2012.06.046](https://doi.org/10.1016/j.ijrobp.2012.06.046), indexed in Pubmed: [22878127](https://pubmed.ncbi.nlm.nih.gov/22878127/).
18. Gee HE, Bignell F, Odgers D, et al. In vivo dosimetric impact of breast tissue expanders on post-mastectomy radiotherapy. *J Med Imaging Radiat Oncol*. 2016; 60(1): 138–145, doi: [10.1111/1754-9485.12403](https://doi.org/10.1111/1754-9485.12403), indexed in Pubmed: [26503758](https://pubmed.ncbi.nlm.nih.gov/26503758/).
19. Ciabattini A, Gregucci F, De Rose F, et al. AIRO Breast Cancer Group . *Tumori*. 2022; 108(2_suppl): 1–144, doi: [10.1177/03008916221088885](https://doi.org/10.1177/03008916221088885), indexed in Pubmed: [36112842](https://pubmed.ncbi.nlm.nih.gov/36112842/).
20. ICRU report 62. Bethesda: International Commission on Radiation Units and Measurements; 1999. Prescribing, recording, and reporting photon beam therapy.
21. Marks LB, Yorke ED, Jackson A, et al. Use of normal tissue complication probability models in the clinic. *Int J Radiat Oncol Biol Phys*. 2010; 76(3 Suppl): S10–S19, doi: [10.1016/j.ijrobp.2009.07.1754](https://doi.org/10.1016/j.ijrobp.2009.07.1754), indexed in Pubmed: [20171502](https://pubmed.ncbi.nlm.nih.gov/20171502/).
22. Bland JM, Altman DG. Statistical methods for assessing agreement between two methods of clinical measurement. *Lancet*. 1986; 1(8476): 307–310, indexed in Pubmed: [2868172](https://pubmed.ncbi.nlm.nih.gov/2868172/).
23. Fleiss JF. The design and analysis of clinical experiments. John Wiley & Sons, New York 1986: Chapter 1.
24. Landis JR, Koch GG. The measurement of observer agreement for categorical data. *Biometrics*. 1977; 33(1): 159–174, indexed in Pubmed: [843571](https://pubmed.ncbi.nlm.nih.gov/843571/).

25. Cordeiro PG, Alborno CR, McCormick B, et al. The impact of postmastectomy radiotherapy on two-stage implant breast reconstruction: an analysis of long-term surgical outcomes, aesthetic results, and satisfaction over 13 years. *Plast Reconstr Surg.* 2014; 134(4): 588-595, doi: [10.1097/PRS.0000000000000523](https://doi.org/10.1097/PRS.0000000000000523), indexed in Pubmed: [25357021](https://pubmed.ncbi.nlm.nih.gov/25357021/).
26. Motwani SB, Strom EA, Schechter NR, et al. The impact of immediate breast reconstruction on the technical delivery of postmastectomy radiotherapy. *Int J Radiat Oncol Biol Phys.* 2006; 66(1): 76-82, doi: [10.1016/j.ijrobp.2006.03.040](https://doi.org/10.1016/j.ijrobp.2006.03.040), indexed in Pubmed: [16765534](https://pubmed.ncbi.nlm.nih.gov/16765534/).
27. Buchholz TA, Strom EA, Perkins GH, et al. Controversies regarding the use of radiation after mastectomy in breast cancer. *Oncologist.* 2002; 7(6): 539-546, doi: [10.1634/theoncologist.7-6-539](https://doi.org/10.1634/theoncologist.7-6-539), indexed in Pubmed: [12490741](https://pubmed.ncbi.nlm.nih.gov/12490741/).
28. Aristei C, Falcinelli L, Bini V, et al. Expander/implant breast reconstruction before radiotherapy: outcomes in a single-institute cohort. *Strahlenther Onkol.* 2012; 188(12): 1074-1079, doi: [10.1007/s00066-012-0231-z](https://doi.org/10.1007/s00066-012-0231-z), indexed in Pubmed: [23111470](https://pubmed.ncbi.nlm.nih.gov/23111470/).
29. Bjöhle J, Onjukka E, Rintelä N, et al. Post-mastectomy radiation therapy with or without implant-based reconstruction is safe in terms of clinical target volume coverage and survival - A matched cohort study. *Radiother Oncol.* 2019; 131: 229-236, doi: [10.1016/j.radonc.2018.07.005](https://doi.org/10.1016/j.radonc.2018.07.005), indexed in Pubmed: [30055939](https://pubmed.ncbi.nlm.nih.gov/30055939/).
30. Mizuno N, Takahashi H, Kawamori J, et al. Determination of the appropriate physical density of internal metallic ports in temporary tissue expanders for the treatment planning of post-mastectomy radiation therapy. *J Radiat Res.* 2018; 59(2): 190-197, doi: [10.1093/jrr/rrx085](https://doi.org/10.1093/jrr/rrx085), indexed in Pubmed: [29342302](https://pubmed.ncbi.nlm.nih.gov/29342302/).
31. Yoon J, Xie Y, Heins D, et al. Modeling of the metallic port in breast tissue expanders for photon radiotherapy. *J Appl Clin Med Phys.* 2018; 19(3): 205-214, doi: [10.1002/acm2.12320](https://doi.org/10.1002/acm2.12320), indexed in Pubmed: [29603586](https://pubmed.ncbi.nlm.nih.gov/29603586/).
32. Aristei C, Kaidar-Person O, Tagliaferri L, et al. The Assisi Think Tank Meeting and Survey of post MAstectomy Radiation Therapy after breast reconstruction: The ATTM-SMART report. *Eur J Surg Oncol.* 2018; 44(4): 436-443, doi: [10.1016/j.ejso.2018.01.010](https://doi.org/10.1016/j.ejso.2018.01.010), indexed in Pubmed: [29422254](https://pubmed.ncbi.nlm.nih.gov/29422254/).
33. Dahn HM, Boersma LJ, de Ruyscher D, et al. The use of bolus in postmastectomy radiation therapy for breast cancer: A systematic review. *Crit Rev Oncol Hematol.* 2021; 163: 103391, doi: [10.1016/j.critrevonc.2021.103391](https://doi.org/10.1016/j.critrevonc.2021.103391), indexed in Pubmed: [34102286](https://pubmed.ncbi.nlm.nih.gov/34102286/).
34. Kaidar-Person O, Vrou Offersen B, Hol S, et al. ESTRO ACROP consensus guideline for target volume delineation in the setting of postmastectomy radiation therapy after implant-based immediate reconstruction for early stage breast cancer. *Radiother Oncol.* 2019; 137: 159-166, doi: [10.1016/j.radonc.2019.04.010](https://doi.org/10.1016/j.radonc.2019.04.010), indexed in Pubmed: [31108277](https://pubmed.ncbi.nlm.nih.gov/31108277/).
35. Lancellotta V, Iacco M, Perrucci E, et al. Comparing four radiotherapy techniques for treating the chest wall plus levels III-IV draining nodes after breast reconstruction. *Br J Radiol.* 2018; 91(1086): 20160874, doi: [10.1259/bjr.20160874](https://doi.org/10.1259/bjr.20160874), indexed in Pubmed: [29474098](https://pubmed.ncbi.nlm.nih.gov/29474098/).
36. Mayorov K, Ali E. Magnitude and dosimetric impact of inter-fractional positional variations of the metal port of tissue expanders in postmastectomy patients treated with radiation. *Phys Imaging Radiat Oncol.* 2020; 16: 37-42, doi: [10.1016/j.phro.2020.09.012](https://doi.org/10.1016/j.phro.2020.09.012), indexed in Pubmed: [33458342](https://pubmed.ncbi.nlm.nih.gov/33458342/).

Table 1. Results of real clinical plans (RP) *in vivo* dosimetry on the 3 patients and RP treatment planning system (TPS) and corrected plan (CP) TPS doses

| Measure point | Film | dose | SD | RP | dose | CP dose |
|---------------|------|------|----|----|------|---------|
| | | | | | | |

| | [Gy] | | [Gy] | |
|---|------|------|------|------|
| 1 | 0.93 | 0.04 | 0.91 | 1.11 |
| 2 | 1.30 | 0.03 | 1.30 | 1.30 |
| 3 | 1.32 | 0.03 | 1.29 | 1.29 |
| 4 | 0.85 | 0.02 | 0.80 | 0.80 |
| 5 | 1.38 | 0.04 | 1.41 | 1.51 |
| 6 | 1.27 | 0.04 | 1.29 | 1.39 |
| | | | | |
| 1 | 1.06 | 0.04 | 1.02 | 1.01 |
| 2 | 1.19 | 0.04 | 1.05 | 1.11 |
| 3 | 1.40 | 0.04 | 1.24 | 1.24 |
| 4 | 1.01 | 0.04 | 1.04 | 1.00 |
| 5 | 1.21 | 0.03 | 1.28 | 1.33 |
| 6 | 1.37 | 0.03 | 1.16 | 1.22 |
| | | | | |
| 1 | 1.07 | 0.03 | 1.01 | 1.01 |
| 2 | 1.26 | 0.03 | 1.06 | 1.12 |
| 3 | 1.31 | 0.05 | 1.25 | 1.25 |
| 4 | 0.98 | 0.04 | 1.03 | 0.99 |
| 5 | 1.17 | 0.04 | 1.26 | 1.32 |
| 6 | 1.37 | 0.03 | 1.17 | 1.23 |

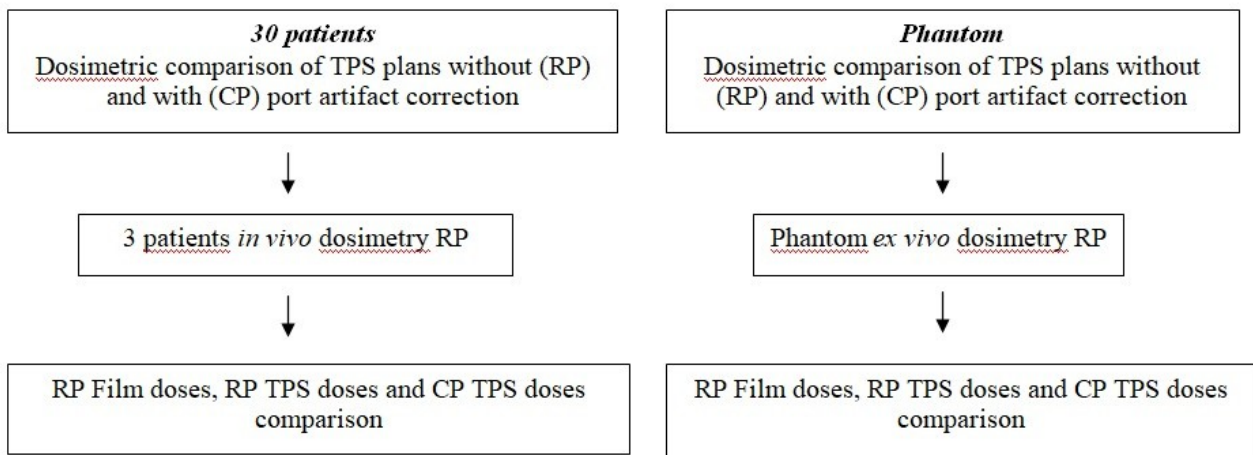
SD — standard deviation

Table 2. Statistical analysis of *in vivo* dosimetry and real clinical plan (RP) and corrected plan (CP) doses

| | Mean \pm SD [Gy] | | Difference in means \pm SD [Gy] | Lower and upper limits of agreement | ICC | CV (%) |
|---|--------------------------|-----|---|--|-------|-----------|
| A | 1.14 \pm 0.16 | A–B | -0.04 \pm 0.06 | -0.15 to 0.08 | 0.968 | 3.9 |
| B | 1.18 \pm 0.17 | A–C | -0.05 \pm 0.10 | -0.24 to 0.14 | 0.908 | 5.8 |
| C | 1.19 \pm 0.17 | B–C | -0.01 \pm 0.11 | -0.23 to 0.20 | 0.887 | 6.6 |

A — doses calculated for the RP; B — doses calculated for the CP; C — doses detected by the films; SD — standard deviation; ICC — intraclass correlation coefficient; CV — coefficient of variation

Figure 1. Study design. TPS — treatment planning system; RP — real plan; CP — corrected plan



Supplementary File

Table S1. Results of real plan (RP) *ex vivo* dosimetry on the phantom and RP and corrected plan (CP) doses

| Measure point | Film dose [Gy] | SD | RP dose [Gy] | CP dose |
|----------------------|-----------------------|-----------|---------------------|----------------|
| 1 | 1.59 | 0.04 | 1.45 | 1.38 |
| 2 | 1.84 | 0.02 | 1.60 | 1.66 |
| 3 | 1.78 | 0.01 | 1.65 | 1.65 |
| 4 | 1.40 | 0.02 | 1.48 | 1.48 |
| 5 | 1.53 | 0.03 | 1.23 | 1.33 |
| 6 | 1.69 | 0.03 | 1.60 | 1.56 |

SD — standard deviation